Order-disorder phase transitions in $NbH_{0.86}$

1998 J. Phys.: Condens. Matter 10 1259

(http://iopscience.iop.org/0953-8984/10/6/009)

J. Phys.: Condens. Matter **10** (1998) 1259–1266. Printed in the UK PII: S0953-8984(98)88119-8

Order–disorder phase transitions in $NbH_{0.86}$

T Plackowski†, N I Sorokina‡ and D Włosewicz†

† Institute of Low Temperature and Structure Research, Polish Academy of Sciences, PO Box 937, 50-950 Wrocław, Poland

‡ Institute of High Pressure Physics, Russian Academy of Sciences, 142092 Troitsk, Moscow Region, Russian Federation

Received 2 October 1997, in final form 18 November 1997

Abstract. Measurements of the electrical resistivity under hydrostatic pressure have been made and an x-ray analysis has been performed for the interstitial alloy $NbH_{0.86}$. The results have been compared with specific heat and thermal expansion results for the same sample. An anomaly in the specific heat observed at 388–394 K was attributed to a phase transition due to the ordering of H atoms. The trapezoidal shape of the anomaly was explained in terms of the equilibrium phase separation occurring within the two-phase region, as in the case of the liquid-solution–vapour transition. At lower temperatures a series of specific heat anomalies at ∼194 K (small), ∼203 K (medium) and ∼216 K (large) was observed and assigned to the subsequent orderings of the H atoms. The smallest anomaly coincides with the change of the Nb-sublattice symmetry which is cubic below and orthorhombic above the temperature at which this anomaly is found and also, with a bend in the curve representing the temperature dependence of the resistivity. The temperature location of this bend has been found to be insensitive to the applied pressure (up to 19.5 kbar). The biggest low-temperature specific heat anomaly coincides with a jump in the relative elongation.

1. Introduction

The hydrides of transition metals have received a great deal of attention—in part because of their technological importance and in part due to the fact that they may help to solve some basic scientific problems. There are two different subsystems in these hydrides—the heavy-metal matrix and the mobile light hydrogen at the interstitial sites—and that is why they are ideal systems to study if one wishes to probe diffusive motion in solids. The deformation (stress-induced) interactions, due to the lattice deformation by the interstitial atoms, and the 'electronic' terms, arising from the screened Coulomb interaction of the protons [1], are the main contributions to the H–H interactions. The extent of the interaction between the interstitial hydrogen atoms as well as that of the H–Nb interactions change with the hydrogen concentration and temperature, resulting in numerous different phase transitions (PTs) in the systems considered, mainly of order–disorder type. These PTs may occur with or without symmetry change of the Nb sublattice. Therefore, the transition metal hydrides may also serve as useful systems to investigate if one wishes to study phase transitions in solids. The phase diagram (PD) of the Nb–H system is complicated, especially for the higher hydrogen concentrations ($H/Nb > 0.7$). Phase diagrams for this system were presented in references [2], [3] and [4]. However, below room temperature the data reveal large discrepancies.

The high-temperature $\beta \rightarrow \alpha'$ PT, of order–disorder type, is well known. In the α'-phase the hydrogen atoms are randomly distributed among the tetrahedral interstitial sites (TISs)

0953-8984/98/061259+08$19.50

of the basic bcc niobium lattice. On cooling, NbH_x (for $x > 0.7$) transforms into the face-centred orthorhombic (fco) β-phase, in which the hydrogen atoms are located at specified TISs in the $(110)_c$ planes of the metal lattice. For the hydrogen concentration $x < 1$, in the β-phase of NbH_x there are vacancies in the hydrogen sublattice. At some temperature below 230 K, the non-stoichiometric β-phase transforms into a λ- or γ-phase with H vacancies ordered on the subset of TISs. The temperatures of these transitions strongly depend on the hydrogen concentration. The λ, γ–β phase boundaries have been studied using resistivity measurements [4], differential thermoanalysis [2] and ultrasound absorption [5]. The γ-phase was reported to be pseudo-cubic on the basis of x-ray diffraction experiments [2, 6]. Electron [7] and neutron [8] diffraction investigations of the λ-phase have shown that this phase is a long-period superstructure in the $[001]_c$ direction (indices are based on the cubic axes). In thin foils of NbH_x at 93 K [7] the fco λ-phase exists over the composition range $x = 0.72$–0.96. The superstructure modulation parameter (δ) was found to be proportional to the number of vacancies in the hydrogen sublattice: $\delta \propto 1 - x$. No evidence for the pseudo-cubic structure previously reported by Pick [6] was observed for any composition. In NbD_x at $T = 77$ K the λ-phase exists over the composition range $x = 0.792$–0.834 for polycrystalline samples and $x = 0.77$–0.84 for single-crystal samples [8].

In the composition range $x = 0.7$–0.9, anomalies in various dependences versus the hydrogen concentration for NbH_x were observed (of the thermopower [9], Knight shift [10] and specific heat [11]) and predicted theoretically [12], so more extensive studies for certain compositions seem likely to be useful as regards achieving an understanding of the H–H interactions in the metal hydrides. It was shown [11, 13, 14] that for high hydrogen concentrations the low-temperature PTs in NbH_x have a number of peculiarities and are strongly dependent on the hydrogen concentration. $NbH_{0.84}$ [14], whose metallic sublattice is fco over the whole temperature range investigated, 15–300 K, displays a series of three peaks in $C_p(T)$ within a very narrow temperature range (of width ~1.5 K) around ~227 K, near the $\lambda \rightarrow \beta$ PT. $NbH_{0.87}$ [13] exhibits two peaks in the $C_p(T)$ curve in the vicinity of the $\lambda \rightarrow \beta$ PT: at 202.5 and at 213.5 K.

The $NbH_{0.86}$ interstitial alloy, which we chose to investigate in this work, has a hydrogen concentration lying between those of the two above-described hydrides. So it may be expected that the hydride $NbH_{0.86}$ should also exhibit a $\lambda \rightarrow \beta$ transition and the features connected with the formation of a λ-phase [2, 4]. According to [7], the hydrogen density wave in a thin foil of $NbH_{0.86}$ may be commensurate with the lattice, with a wavelength of $\frac{16}{3}a[001]_c$.

In this paper we present the results of the various experiments performed on $NbH_{0.86}$. Specific heat data were presented in reference [11] for this alloy, which was there just representing a member of the NbH_x system; now we analyse them in more detail. Thermal expansion data for this sample have also been published in reference [15]. In order to establish more firmly the character of the low-temperature phase transitions in $NbH_{0.86}$, we performed measurements of the electrical resistivity under high hydrostatic pressure (4.2–300 K, $p \leqslant 19.5$ kbar) as well as x-ray powder analysis (15–300 K). In the present paper we present an analysis of all of the above-mentioned results.

2. Experimental procedure

The samples of $NbH_{0.86}$ were prepared from a niobium single crystal with a ratio $\rho(300\ \text{K})/\rho(10\ \text{K}) = 56$ by the gas saturation method at $p_{H_2} \leqslant 5$ atm and $T \sim 1120$ K (holding time: ~2 h). The content of hydrogen was determined within 1% accuracy [15]. The experimental density of this sample at 300 K amounts to 7.62 ± 0.01 g cm^{-3} whereas

the calculated x-ray density is equal to 7.57 ± 0.012 g cm^{-3}. Samples from the same batch were used for all of the experiments. The value of $\rho(300\ \mathrm{K})/\rho(4.2\ \mathrm{K})$ can be as high as $\sim$13. The x-ray investigations were accomplished with the help of a D5000 Siemens diffractometer. The low-temperature PT has been studied under hydrostatic pressure up to 19.5 kbar (as measured at $T = 192$ K) in a fixed-pressure vessel [16] by means of electrical resistivity measurements with an absolute error of 3%. The pressure was measured by a calibrated manganin sensor. The errors in the pressure and temperature determination amount to ± 0.2 kbar and 0.2 K, respectively, over the whole range investigated. The specific heat measurements were performed in a fully automated adiabatic calorimeter using both the heat-pulse and continuous methods [11, 17]. The mass of the $NbH_{0.86}$ sample used for the calorimetry was 353 mg. The relative elongation was measured with a L75/80 Linseis dilatometer with cooling and heating rates of 2 K min^{-1} [15].

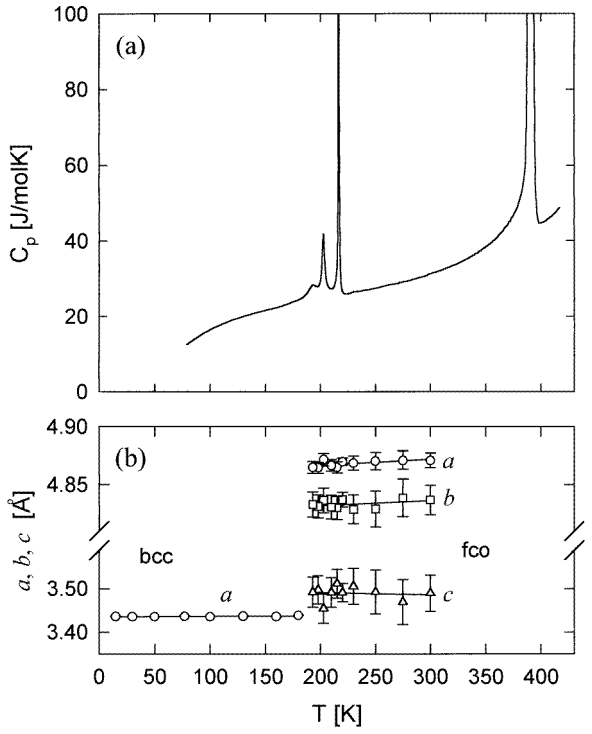

Figure 1. (a) The specific heat of $NbH_{0.86}$ over the temperature range 80–430 K. (b) The unit-cell parameters of the Nb sublattice in $NbH_{0.86}$ over the temperature range 15–300 K.

3. Results and discussion

The specific heat, C_p, of $NbH_{0.86}$ over the whole temperature range investigated, 80–430 K, as well as the unit-cell parameters for the temperature range 15–300 K are shown in figures 1(a) and 1(b). Several anomalies at temperatures $T \sim 194$ K, $T \sim 203$ K, $T \sim 216$ K and in the range 388–394 K are visible in the $C_p(T)$ curve. They are attributable to the phase transitions corresponding to the stepwise ordering of the hydrogen atoms with decreasing temperature and will be discussed below. At temperatures above 250 K (excluding that of the high-temperature anomaly), a continuous increase of C_p with temperature is observed, contrary to the prediction of the Dulong–Petit law. This may be ascribed to the additional specific heat contribution due to the high hydrogen diffusivity [13].

In the temperature region investigated by means of x-ray powder diffraction (1–300 K)—see figure 1(b)—only one $C_p(T)$ anomaly (the lowest one, at $T \sim 194$ K) can be related to a change of the Nb-sublattice structure. This is a transformation from the cubic (bcc) structure into the fco structure accompanied by the doubling of the unit cell. No evidence for a second-order-type transition at 100 K, reported in [5] for polycrystalline $NbH_{0.86}$, was observed by means of the $C_p(T)$ and x-ray measurements.

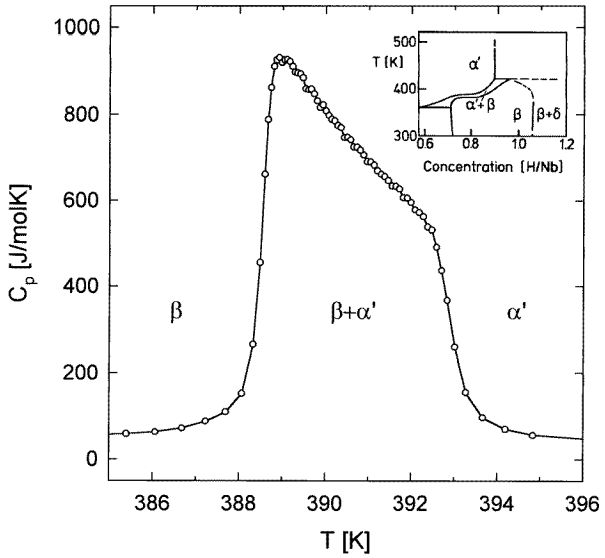

Figure 2. The specific heat of $NbH_{0.86}$ in the vicinity of the $\beta \rightarrow \alpha'$ phase transition. The inset shows a part of the phase diagram of the NbH_x system near the $\beta \rightarrow \alpha'$ PT (taken from reference [3]).

3.1. The high-temperature phase transition

The anomaly in $C_p(T)$ in the 388–394 K range is associated with the $\beta \rightarrow \alpha'$ order–disorder phase transition [2, 4]. This trapezoidal, relatively wide ($\sim$6 K in width) and very high (more than one order of magnitude higher than the background) peak is shown in figure 2. The onset (388 K) and the end (394 K) of the anomaly are very distinct and agree well with the boundaries of the coexistence region of the β- and α'-phases in the phase diagram for the hydrogen concentration $x = 0.86$ (see the inset in figure 2). This suggests that in the temperature range of the two-phase region an equilibrium phase separation occurs in the sample into α'- and β-phases which have slightly different hydrogen contents. This difference should obviously be proportional to the slope of the $\beta/(\beta+\alpha')$ and $(\beta+\alpha')/\alpha'$ boundaries in the phase diagram. The literature data indicate an extremely high diffusivity of hydrogen in metals and therefore very short mean residence times of H atoms at TISs ($\sim 10^{-9}$ s for $NbH_{0.9}$ at $\sim$400 K [2]). Thus, the diffusion coefficient of hydrogen seems to be high for thermal equilibrium of both of the phases to be maintained (i.e. the α'-phase, which is less rich in hydrogen, and the β-phase, which is more hydrogenated) during the relatively slow $C_p(T)$ measurements. The asymmetric shape of the peak may be comprehensible, since the distance between the $\beta/(\beta+\alpha')$ and $(\beta+\alpha')/\alpha'$ lines in the phase diagram grows with the increasing hydrogen concentration. Therefore, near the $\beta/(\beta+\alpha')$ line, more β-

phase is transformed into α'-phase per temperature interval than near the $(\beta + \alpha')/\alpha'$ line, and the left-hand side of the $C_p(T)$ anomaly is higher.

The entropy jump at this transition, $\Delta S = 8.90$ J mol^{-1} K^{-1}, was calculated by measuring the area under the peak for the $C_p(T)/T$ curve (including the rise of the specific heat visible from ~330 K). In the bcc Nb sublattice, six equivalent TISs per Nb atom may be distinguished, which may be regarded as $6/x$ degrees of freedom per hydrogen atom in NbH_x. The entropy of the blocking of n TISs (or, equivalently, the freezing of n/x degrees of freedom for x hydrogen atoms per Nb atom) may be calculated as $\Delta S/R = x \ln(n/x)$ (R is the gas constant). Thus, the value of ΔS measured for $NbH_{0.86}$ may be interpreted as the blocking of $n \approx 3.0$ TISs per bcc unit cell of the Nb sublattice (i.e. approximately three TISs became forbidden for the hydrogen atoms).

It should be noted that the temperatures of the onset (388 K) and the end (406 K) of this $\beta \rightarrow \alpha'$ PT determined from the jump in the relative elongation measured for the same sample of $NbH_{0.86}$ [15] agree quite well with the boundaries of the $\beta \rightarrow \alpha'$ PT obtained from calorimetric data. The jump of the relative elongation along the $(100)_c$ axis in the $\beta \rightarrow \alpha'$ PT amounts to $\Delta l/l_0 \approx 0.026\%$.

3.2. Low-temperature phase transitions

Figure 3 shows the behaviour of various physical quantities near the low-temperature transitions. The enlargement of the low-temperature $C_p(T)$ anomalies is presented in figure 3(a). Three peaks of different heights are visible at 193.8, 202.6 and 216.25 K. The latter is the most pronounced and is two orders of magnitude higher than the background. The entropies, ΔS, associated with the particular peaks were assessed by means of numerical deconvolution as 0.34, 0.34 and 1.1 J mol^{-1} K^{-1} for the peaks in order of increasing temperature, respectively. Since Lorentzian shapes were arbitrarily assumed for the peaks in this method, the entropies obtained should be regarded as rough estimates only. The vertical, dotted lines in figure 3 denote the positions of the $C_p(T)$ peaks.

The existence of a phase transition below room temperature was confirmed by the x-ray powder measurements carried out on the $NbH_{0.86}$ sample while the sample was heated step by step from 15 to 300 K. Figure 3(b) shows the variation of the unit-cell parameters a, b and c of the heavy-Nb-atom sublattice, indicating the existence of cubic structure up to ~180 K (the γ-phase) and the fco-type structure above this temperature. In figure 3(c) the temperature variation of the unit-cell volume V is shown (double the volume is presented for the cubic structure, because the fco unit cell contains twice as many atoms as the cubic cell). The data for $T = 180$ K could also be fitted assuming cubic or orthorhombic symmetry, so the transformation seems to occur over a temperature range (the hatched regions in figures 3(b) and 3(c)) or to be of continuous character.

Figure 3(d) presents the results of resistivity measurements made under hydrostatic pressure taken along the direction $[100]_c$. No hysteresis was observed for measurements made with increasing and decreasing temperature. The pressure in the measurement vessel was changing slightly with changing temperature, so the pressure values were presented for the fixed temperature $T = 192$ K. The extent of the fold-shaped anomaly visible for $p = 0$ is highlighted with a horizontal arrow and a hatched area. The position of the bend in the $\rho(T)$ curves seems to be independent of the pressure, whereas the anomaly becomes more and more hard to discern with increasing pressure.

The relative elongation of $NbH_{0.86}$, $\Delta l/l_0$ ($l_0 = l$ at 300 K), along the $[100]_c$ axis of the Nb sublattice over the temperature range 165–245 K is presented in figure 3(e). A jump of the magnitude $\Delta(\Delta l/l_0) \approx 2.4 \times 10^{-4}$ with a large hysteresis was observed: it occurred

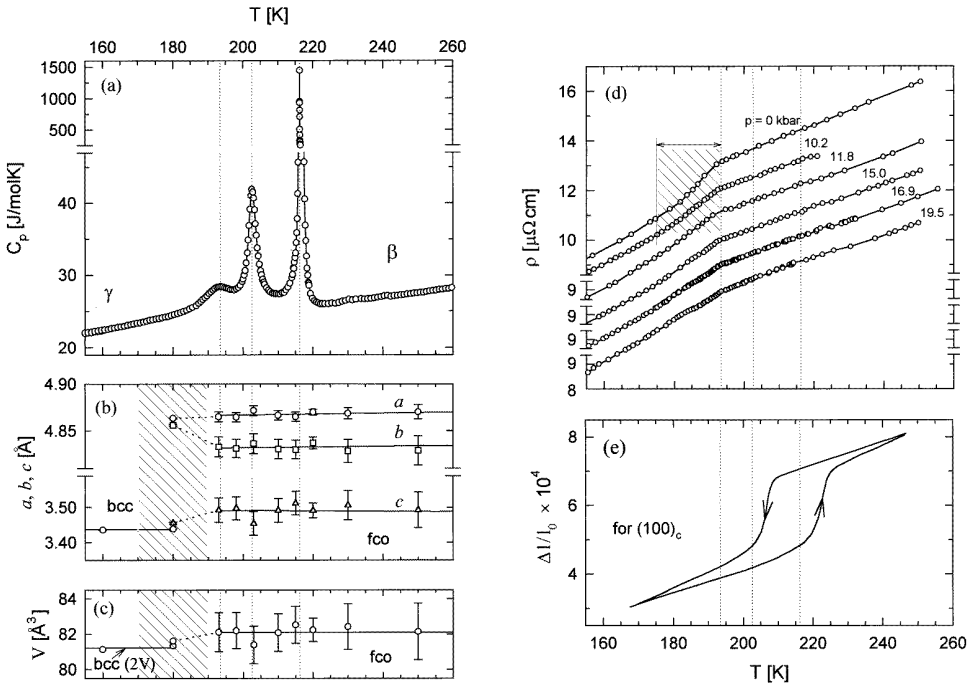

Figure 3. The temperature dependences of various physical quantities near the $\gamma \rightarrow \beta$ PT for $NbH_{0.86}$. The vertical dotted lines denote the positions of the peaks in the $C_p(T)$ curve. (a) The specific heat. (b) Cell parameters (the vertical error bars denote the model matching error). (c) The volume of the unit cell. (The hatched regions in (b) and (c) indicate the regions of possible coexistence of two phases.) (d) The electrical resistivity under hydrostatic pressure (the horizontal arrow and the hatched region indicate the extent of the anomaly for lower pressures). (e) The relative elongation in the direction of the $[100]_c$ axis in the Nb-atom lattice.

at 206 K during cooling and at 223 K during heating.

We would like to emphasize that the phase diagrams for the NbH_x system presented in references [2], [3] and [4] suggest that at low temperatures for $x = 0.86$ several phase boundaries exist, surrounding either single- or two-phase regions. Since the diffusion coefficient of hydrogen is significantly lower at low temperature (the diffusion coefficients for $NbH_{0.9}$ at the temperatures 400 K and 250 K differ by two orders of magnitude [2]), the phase boundaries of the two-phase regions may not be so easy to discern in the $C_p(T)$ curve as they are in the case of the anomaly related to the $\beta \rightarrow \alpha'$ phase transition. Therefore, it is difficult to decide, without any additional knowledge, whether a particular peak in $C_p(T)$ should be attributed to a phase transition that passes through a two-phase region or one that does not.

The smallest anomaly in $C_p(T)$, at ∼194 K (the peak temperature), with the associated entropy jump $\Delta S = \sim 0.34$ J mol^{-1} K^{-1}, coincides well with the anomaly in $\rho(T)$ and with the change of the Nb-sublattice symmetry, as detected by the x-ray measurements. The analysis of the structural data suggests that this may be a phase transition which commences on passing through a two-phase region. The agreement of the extent of the $\rho(T)$ anomaly region (∼175–194 K—see the horizontal arrow in figure 3(d)) with structural data (see the hatched area in figure 3(b)) confirms the above suggestion. Thus, this transition should be regarded as of first-order type. The volume jump at this transition observed in x-ray

diffraction data is less than the measurement error, and no effect was noticed in the $\Delta l/l_0$ curve. This, according to the Clausius–Clapeyron equation, agrees well with measured $dT_{PT}/dp \approx 0$ value. It is also noteworthy that for this PT the peak in $C_p(T)$ is located at the end of the two-phase region. This asymmetry seems to be connected, in contrast to the case for the $\beta \rightarrow \alpha'$ PT, with the dynamics of the hydrogen reordering due to its weaker diffusion at low temperatures.

The PTs connected with the anomalies at ∼203 K and ∼216 K are isostructural—the niobium matrix still has the fco structure, like the β-phase. Thus, they seem to be connected with ordering in the H sublattice only. The entropy jumps amount to ∼0.34 and ∼1.1 J mol^{-1} K^{-1}, respectively. No anomalies in the resistivity and x-ray data were detected above 192 K; only in the relative elongation was a hysteretic jump observed near the temperature at which there was the greatest anomaly in the specific heat. It may be proposed that the anomaly appearing in $\Delta l/l_0$ at 223 K (beginning at ∼215 K) observed upon heating corresponds to the anomaly at ∼216 K in $C_p(T)$. Since the dynamics of the low-temperature PT seems to be important, it should be noticed that the rate of the temperature change was ∼4 times higher for the relative-elongation experiment than for the specific heat experiment. To sum up, the transformation at ∼216 K should also be regarded as of first-order type, but no conclusion may be reached regarding the PT at ∼203 K.

4. Conclusions

The data concerning the specific heat, x-ray powder diffraction, resistivity under hydrostatic pressure and relative elongation for $NbH_{0.86}$ were analysed. The $C_p(T)$ measurements for $NbH_{0.86}$ revealed a series of anomalies at temperatures $T \sim 194$ K, $T \sim 203$ K, $T \sim 216$ K and $T \sim 388$–394 K. The x-ray powder analysis carried out for the range 15–300 K revealed that the structure of the Nb sublattice is of the bcc type below ∼180 K at least down to 15 K (the γ-phase) and of fco type above ∼180 K.

The high diffusion coefficient of hydrogen for the NbH_x system and the shape of the anomaly at 388–394 K in $C_p(T)$ provided evidence that in the two-phase region between the β- and α'-phase areas a separation occurs into phases less rich (α') and richer (β) in hydrogen, both of which remain in thermodynamic equilibrium over the whole two-phase region. Such behaviour, typical for liquid-solution–vapour transitions, is seldom observed in the solid state. The value of the measured entropy of the $\beta \rightarrow \alpha'$ PT suggests that in the β-phase about three of a total six TISs existing in the bcc lattice per Nb atom become blocked.

The interpretation of the series of three anomalies in $C_p(T)$ at low temperatures is more difficult, because only the anomaly of the smallest height (at ∼194 K) coincides with a structure change observable by means of x-ray powder diffraction. The rearrangement of Nb atoms causes a bend in the $\rho(T)$ curve (at ∼175–194 K), whose temperature location has been found to be insensitive to the applied pressure. It is suggested that this PT is of first-order type, and commences on passing through a two-phase region. The second anomaly in $C_p(T)$ (at ∼203 K) is not associated with any effect in either the $\rho(T)$ or the $\Delta l(T)/l_0$ curves, or in the x-ray data, while the biggest anomaly at (∼216 K) may be attributed to a highly hysteretic jump in the relative-elongation curve. This intimates the first-order type of this transition. The two phases existing between these three low-temperature PTs exhibit the same symmetry of the Nb sublattice as the β-phase. The values of the entropy jumps assessed that are associated with these three transitions indicate that the degree of ordering in the hydrogen subsystem is the highest for the PT near ∼216 K, despite the fact that this is the PT near ∼194 K which is tied in with metal-sublattice rearrangement.

As was shown in the introduction, the $NbH_{0.86}$ alloy has a hydrogen concentration that lies in the range in which anomalies in the compositional dependences of various quantities have been observed for the NbH_x system [9–11]. In fact, a significant asymmetry may be observed when comparing the result for $NbH_{0.86}$ with those for the NbH_x alloys with slightly higher or lower hydrogen concentrations. The specific heat data for $NbH_{0.86}$ are much more similar to the respective data for $NbH_{0.87}$ than to those for $NbH_{0.84}$ [13, 14]. However, despite the different shapes of the observed anomalies, the total entropy calculated from the $C_p(T)$ curves, separately for low- and high-temperature PTs, is almost constant for all three compositions: $x = 0.84$, 0.86 and 0.87 [11]. The relative-elongation and pressure data for the NbH_x system are still incomplete. For $NbH_{0.87}$ only the relative elongation has been measured [18] at low temperatures, showing a jump of similar hysteresis to that for $NbH_{0.86}$, but shifted by 7 K towards lower temperatures. The electrical resistivity for $NbH_{0.84}$ [19] shows a step at ∼220 K which is shifted to ∼247 K by a hydrostatic pressure of 19.6 kbar. This is in contrast with the results presented for $NbH_{0.86}$, for which the resistivity anomaly has been found to be insensitive to pressure. However, the Clausius–Clapeyron relation is fulfilled for both of the compositions $x = 0.86$ and $x = 0.84$ [14].

In conclusion, the NbH_x system may serve as a good introduction to studying phase transitions in the solid state. Strong H–H interactions make the phase diagram of this system rich in various features, including two-phase regions. It appears that the strong temperature dependence of the hydrogen diffusion through the heavy-metal sublattice makes it possible to execute the temperature runs of an experiment (investigating the specific heat in our case) through the two-phase regions with ($\beta \rightarrow \alpha'$) or without ($\gamma \rightarrow \beta$) maintaining the thermal equilibrium of the phases. It should also be stressed that the specific heat seems to be the most sensitive detector of phase transitions in metal hydrides ($NbH_{0.86}$ is a prime example of a compound for which some PTs manifest themselves only in anomalies of some of the physical quantities). At low temperatures, however, the precise determination of the phase boundaries is hampered due to the low hydrogen diffusivity and the resulting large hysteretic effects (see the results for the relative elongation).

References

[1] Vaks V G and Orlov V G 1988 *J. Phys. F: Met. Phys.* **18** 883
[2] Alefeld G and Völkl J (ed) 1978 *Hydrogen in Metals* Parts I and II (Berlin: Springer)
[3] Köbler U and Welter J M 1982 *J. Less-Common Met.* **84** 225
[4] Welter J M and Shondube F 1983 *J. Phys. F: Met. Phys.* **13** 529
[5] Melik-Shakhnasarov V A, Bydlinskaya J N, Naskidashvili J A, Arabajian N L and Chachanidze R V 1981 *Zh. Eksp. Teor. Fiz.* **81** 314
[6] Pick M A 1973 Strukturelle Phasenübergänge im NbH-System *KFA Jülich Technical Report* Jül-951-FF
[7] Makenas B J and Birnbaum H K 1982 *Acta Metall.* **30** 469
[8] Brun T O, Kajitani T, Mueller M H, Westlake D G, Makenas B J and Birnbaum H K 1979 *Proc. Modulated Structure Mtg (Kailua-Kona, Hawaii); AIP Conf. Proc.* **53** 397
[9] Sorokina N I 1989 *Fiz. Tverd. Tela* **31** 123
[10] Ueda T, Hayashi S and Hayamizu K 1993 *Solid State Commun.* **87** 429
[11] Plackowski T, Włosewicz D and Sorokina N I 1995 *Physica* B **212** 119
[12] Vaks V G and Orlov V G 1989 *J. Phys.: Condens. Matter* **1** 9085
[13] Sorokina N I, Włosewicz D and Plackowski T 1993 *J. Alloys Compounds* **194** 141
[14] Włosewicz D, Plackowski T and Sorokina N I 1995 *Physica* B **212** 113
[15] Sorokina N I, Basargin O V and Savin B I 1991 *Fiz. Tverd. Tela* **33** 3565
[16] Itskevich E S, Voronovsky A N, Gavrilov A F and Sukhoparov V A 1966 *Prib. Tekh. Eksp.* **6** 161
[17] Włosewicz D, Plackowski T and Rogacki K 1993 *Cryogenics* **32** 265
[18] Sorokina N I, Basargin O V and Savin B I 1993 *Fiz. Tverd. Tela* **35** 2958
[19] Sorokina N I and Evdokimova V V 1987 *Fiz. Tverd. Tela* **29** 218